

In each case 4 Si-O, 4 C-O, and 12 C-H bonds are broken.

In Figure 1 the periodic trends of h_0 and h_i are displayed. The values of h increase in general with increasing difference in electronegativity from oxygen, as might be expected. For the alkali and, to a lesser extent, the alkaline earth elements, there is considerable difference between h and h_0 and the values of h_0 do not show such simple trends across the periodic table. What is striking is that the difference $h - h_0$ for a given group increases monotonically with atomic number. For Li, Na, and K this difference is 43, 83, and 118 kJ mol⁻¹, and for Be, Mg, Ca, Ba, and Sr it is 4, 7, 26, 50, and 62 kJ mol⁻¹, respectively. It is thought that the differences reflect the increasing importance of nonbonded repulsions between the metal atoms in cation-rich compounds such as especially the

binary alkali-metal oxides in which each oxygen is coordinated by eight metal atoms. (Compare an oxide such as Na₂SiO₃ in which each oxygen is surrounded by four metal atoms.) Further discussion of this point is better deferred for another occasion.

In conclusion, the main result of this work might be emphasized. It is that the heat of atomization (bond energy) of complex oxides can be accurately represented as a sum of equivalent-bond enthalpies that apparently do not depend on crystal structure.

Acknowledgment. This work is part of a program of research into crystal chemistry supported by the National Science Foundation (Grant DMR-8119061).

Communications

Synthesis and Structural Characterization of Bis(tetraphenylphosphonium) Bis(diethyldithiocarbamate)bis(thiophenolato)tetrakis(μ_3 -sulfido)tetraferate(2II,2III), (Ph₄P)₂[Fe₄S₄(SPh)₂(Et₂dtc)₂]. A "Cubane" Type Cluster with Mixed Terminal Ligands and Two Different Modes of Ligation on the Fe₄S₄ Core

Sir:

Synthetic analogues for the 4Fe-4S centers in non-heme-iron proteins are well-known. The molecular and electronic structures and reactivities of various of these complexes have been studied extensively mainly by Holm, Ibers, and co-workers.¹ In the structurally characterized clusters of this type the iron atoms in the Fe₄S₄ cores are tetrahedrally coordinated by three of the triply bridging sulfide ions and a terminal RS⁻ (R = alkyl or aryl) or Cl⁻ ligand. Mixed terminal ligand clusters of the type [Fe₄S₄(SR)_{4-n}X_n]²⁻ ($n = 1-4$; X = Cl⁻, OAc⁻) have been identified in solution and characterized by electronic spectroscopy, electrochemical studies, and ¹H NMR spectroscopy.² Interest in the latter type of complexes derives from the possible presence of such species in certain metalloproteins which contain 4Fe-4S centers with unusual Mössbauer spectra and electronic spin ground states. In the oxidized 4Fe-4S "P clusters" of nitrogenase, which show Mössbauer spectra consistent with two distinct iron sites and an uncommon electronic-spin ground state ($S \geq 3/2$),³ significant differences in the ligation of the Fe₄S₄ cores may account for the unique spectral properties. It has been suggested³ that such differences in ligation could include expansion to five-coordination for the iron atoms or replacement of thiolate terminal ligands by other nucleophiles.

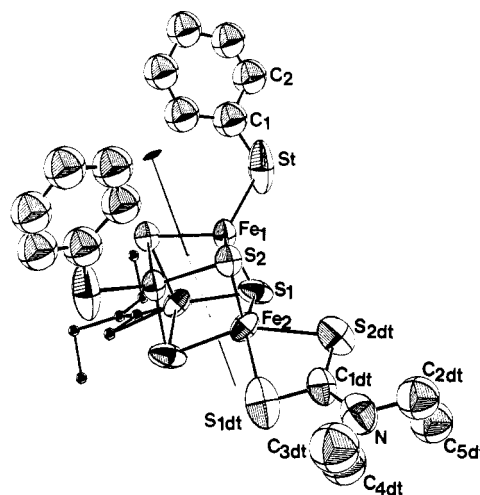


Figure 1. Structure of the [Fe₄S₄(SPh)₂(Et₂dtc)₂]²⁻ anion showing the atom-labeling scheme. Thermal ellipsoids are drawn by ORTEP¹⁸ and represent the 50% probability surfaces. The ellipsoids for one of the Et₂dtc ligands have been drawn with artificially small temperature factors for clarity.

Recently we reported⁴ briefly on the isolation and structure determination of [Fe₄S₄(SPh)₂Cl₂]²⁻, and suggested the possible use of this molecule in the synthesis of other mixed terminal ligand clusters. In this communication we report on the synthesis and structural characterization of [Fe₄S₄(SPh)₂(Et₂dtc)₂]²⁻ (I), a new mixed terminal ligand cluster that shows differences in ligation for the iron atoms in the Fe₄S₄ core.⁵

The reaction of (Ph₄P)₂[Fe₄S₄(SPh)₂Cl₂] with sodium diethyldithiocarbamate, NaEt₂dtc, in acetonitrile at ambient temperature, in a 1:2 molar ratio, proceeds readily. Following filtration of the reaction mixture and addition of ether to incipient crystallization, black crystals of I form and are isolated in ~90% yield. Anal. Calcd for Fe₄S₁₀P₂C₇₀N₂H₇₀ ($M_r = 1.544$): Fe, 14.51; S, 20.73; C, 54.42; N, 1.81; H, 4.53. Found: Fe, 14.68; S, 20.03; C, 55.37; N, 1.88; H, 4.72. The synthesis of I (in ~80% yield) can be accomplished also by

- (1) (a) Holm, R. H. *Acc. Chem. Res.* **1977**, *10*, 427 and references therein. (b) Laskowski, E. J.; Frankel, R. B.; Gillum, W. O.; Papaefthymiou, G. C.; Renaud, J.; Ibers, J. A.; Holm, R. H. *J. Am. Chem. Soc.* **1978**, *100*, 5322. (c) Ibers, J. A.; Holm, R. H. *Science (Washington, D.C.)* **1980**, *209*, 223.
- (2) (a) Johnson, R. W.; Holm, R. H. *J. Am. Chem. Soc.* **1978**, *100*, 5338. (b) Que, L., Jr.; Bobrik, M. A.; Ibers, J. A.; Holm, R. H. *Ibid.* **1974**, *96*, 4168.
- (3) (a) Münck, E.; Rhodes, H.; Orme-Johnson, W. H.; Davis, L. C.; Brill, W. J.; Shah, V. K. *Biochim. Biophys. Acta* **1975**, *400*, 32. (b) Zimmermann, R.; Münck, E.; Brill, W. J.; Shah, V. K.; Henzl, M. T.; Rawlings, J.; Orme-Johnson, W. H. *Ibid.* **1978**, *537*, 185. (c) Huynh, B. H.; Henzl, M. T.; Christner, J. A.; Zimmermann, R.; Orme-Johnson, W. H.; Münck, E. *Ibid.* **1980**, *623*, 124. (d) Münck, E. In "Mössbauer Spectroscopy and Its Chemical Applications"; Stevens, J. G., Shenoy, G. K., Eds.; American Chemical Society: Washington, DC, 1981; Adv. Chem. Ser. No. 194, p 305.

(4) Coucouvanis, D.; Kanatzidis, M.; Simhon, E.; Baenziger, N. C. *J. Am. Chem. Soc.* **1982**, *104*, 1874.

(5) The synthesis of the [Bu₄N][Fe₄S₄(Et₂dtc)₄] and Fe₄S₄(Et₂dtc)₄ complexes has been accomplished recently. The magnetic and Mössbauer properties of these complexes have been investigated: Silverthorn, W. E.; Wells, F. V.; Wickman, H. H., submitted for publication in *Inorg. Chem.* Wickman, H. H., private communication.

Table I. Selected Structural Parameters of Some Clusters Containing the Fe_4S_4 Cores^a

	$[\text{Fe}_4\text{S}_4(\text{SPh})_2(\text{Et}_2\text{dtc})_2]^{2-}$	$[\text{Fe}_4\text{S}_4(\text{SPh})_4]^{2-}$ ^b	$[\text{Fe}_4\text{S}_4(\text{S}_2\text{C}_2(\text{Cl}^+)_2)_4]^{2-}$ ^b
Bond Lengths, Å			
Fe(1)–Fe(1)'	2.733 (3)	2.733 (2)	3.19 (2)
Fe(2)–Fe(2)'	3.053 (3)	2.727 (2)	3.26 (2)
Fe(1)–Fe(2)	2.780 (2)	2.745 (3)	2.77 (3)
Fe(1)–Fe(2)'	2.779 (2)	2.732 (2)	2.68 (10)
Fe(1)–S(1)	2.217 (4)	2.263 (3)	2.17 (4)
Fe(2)–S(2)	2.254 (3)	2.271 (10)	2.14 (2)
Fe(1)–S(2)	2.297 (3)	2.306 (3)	2.23 (2)
Fe(1)–S(2)'	2.307 (3)	2.298 (5)	2.27 (4)
Fe(2)–S(1)	2.309 (4)	2.285 (15)	2.30 (9)
Fe(2)–S(1)	2.364 (4)	2.297 (3)	2.26 (3)
Fe(1)–S _t	2.281 (4)	2.260 (3)	
Fe(2)–S(1) _{dt}	2.552 (4)		
Fe(2)–S(2) _{dt}	2.436 (4)		
Angles, deg			
Fe(2)–Fe(1)–Fe(2)'	66.63 (6)	59.72 (6)	72 (1.5)
Fe(1)–Fe(2)–Fe(1)'	58.89 (6)	59.86 (6)	73.5 (1.5)
Fe(2)–Fe(1)–Fe(1)'	60.53 (5)	59.83 (6)	52 (2)
Fe(2)–Fe(1)–Fe(1)'	60.58 (5)	60.32 (7)	55 (1)
Fe(1)–Fe(2)–Fe(2)'	56.66 (5)	60.39 (7)	55 (1)
Fe(1)–Fe(2)–Fe(2)'	56.71 (5)	60.13 (25)	53 (2)
S(1)–Fe(2)–S(1)	96.44 (17)	105.2 (5)	
S(2)–Fe(1)–S(2)'	104.30 (17)	105.3 (1)	

^a The numbering scheme, shown in Figure 1 for I, applies in an analogous fashion for all the compounds in the table. ^b Average values of bond length and bond angle pairs that in the structure of I are related by the crystallographic twofold axis.

the reaction of $(\text{Ph}_4\text{P})_2[\text{Fe}_4\text{S}_4(\text{SPh})_4]$ with NaEt_2dtc in CH_3CN under similar reaction conditions. The ^1H NMR spectrum of I in CD_3CN displays isotropically shifted resonances for the ortho, para, and meta protons of the PhS^- ligands, respectively, at 5.72, 5.10, and 8.18 ppm (vs. Me_4Si at 300 K). This pattern is similar to the one observed for the PhS^- ligands in the $[\text{Fe}_4\text{S}_4(\text{SPh})_4]^{2-}$ complex⁶ (at 5.70, 5.05, and 8.25 ppm; $T = 300$ K) and arises as a result of dominant contact interactions. The resonances for the CH_2 and CH_3 protons of the Et_2dtc^- ligands are observed as broad signals at 6.94 and 1.19 ppm, respectively. The visible spectrum of this paramagnetic⁷ compound is characterized by an absorption at 420 nm (ϵ 12 500).

In the crystal structure of I⁸ the $[\text{Fe}_4\text{S}_4(\text{SPh})_2(\text{Et}_2\text{dtc})_2]^{2-}$ anion is located on a crystallographic twofold axis and contains a distorted central Fe_4S_4 core (Figure 1). Unlike similar cores in $[\text{Fe}_4\text{S}_4(\text{SPh})_4]^{2-}$ ^{2b} and $[\text{Fe}_4\text{S}_4(\text{SCH}_2\text{Ph})_4]^{2-}$,⁹ which show approximate D_{2d} symmetry, the Fe_4S_4 in I does not show any approximate symmetry higher than the crystallographically

imposed C_2 symmetry (Table I). The Fe–Fe distances divide into three sets (1 + 1 + 4), the Fe–S bonds into five sets (2 + 2 + 2 + 2 + 4), and the Fe–Fe–Fe angles into four sets (2 + 2 + 4 + 4). The two edges of the Fe_4 "tetrahedron" that are perpendicular to the twofold axis differ in length by a significant amount. The short Fe(1)–Fe(1)' distance (2.733 (3) Å) between the Fe atoms coordinated by the PhS^- ligands is virtually identical with the Fe–Fe distances in $[\text{Fe}_4\text{S}_4(\text{SPh})_4]^{2-}$. The "long" Fe(2)–Fe(2)' distance (3.053 (3) Å), associated with the iron atoms coordinated by the Et_2dtc^- ligands, accounts for the significant deviations from 60° of the Fe(2)–Fe(1)–Fe(2)', Fe(1)–Fe(2)–Fe(2)', and Fe(1)–Fe(2)–Fe(2)' angles at 66.63 (6), 56.66 (5), and 56.71 (5)°, respectively (Figure 1). These angular distortions underscore the deviations of the Fe_4 polyhedron from tetrahedral geometry toward a "butterfly" geometry. The possible C_{2v} symmetry of this geometry is not realized because of a significant asymmetry in the Fe(2)–S(1)–Fe(2)–S(1)' rhombic unit. This asymmetry very likely is a result of the unequal Fe(2)–S(1)–(Et₂dtc) bonds, thus the longer Fe(2)–S(1)' bond (2.364 (4) Å) is located trans to the short Fe(2)–S(Et₂dtc) bond (2.436 (4) Å), while the shorter Fe(2)–S(1) bond (2.309 (4) Å) is found trans to the long Fe(2)–S(Et₂dtc) bond (2.552 (4) Å) (Figure 1).

The Fe(1) sites in I, with terminal PhS^- ligands and tetrahedral, FeS_4 , coordination are very similar to the iron sites in $[\text{Fe}_4\text{S}_4(\text{SPh})_4]^{2-}$.^{2b} The Fe(2) sites with terminal Et_2dtc^- ligands show distorted square-pyramidal, FeS_5 , coordination. The four S(1)–Fe(2)–S_{eq} angles range from 100.67 to 112.80° with a mean value of 105.4 (5.0)°, and the iron is out of the equatorial plane¹⁰ and toward S(1) by 0.59 (1) Å. The Fe(2)–S(1) vector deviates from the normal to the equatorial plane by 5°. By comparison, the Cl–Fe–S angle in the square-pyramidal $\text{ClFe}(\text{Et}_2\text{dtc})_2$ complex¹¹ is 105.4 (3)° and the iron is out of the equatorial plane by 0.62 Å. The equatorial Fe(2)–S bonds show unequal lengths in the range from 2.309 to 2.552 Å. The Fe(2)–S bonds associated with the Et_2dtc ligand in I are significantly longer than either the Fe(III)–S bonds in $\text{ClFe}(\text{Et}_2\text{dtc})_2$ (2.300 (10) Å) or the Fe(II)–S bonds in the $[\text{Fe}^{\text{II}}(\text{Et}_2\text{dtc})_2]_2$ dimer¹² (2.404 (2) and 2.453 (2) Å). The Fe(2)–S(Et₂dtc) bonds in I are quite similar to the Fe(III)–S bonds in $\text{Fe}(\text{salen-pyrroldtc})$ ¹³ (2.452 (2) and 2.566 (2) Å). It has been suggested¹³ that in the latter, both sulfur atoms of the pyrroldtc⁻ ligand may occupy one coordination site. A similar suggestion could be advanced for the Et_2dtc ligands in I.¹⁴ The only other example of a $[\text{Fe}_4\text{S}_4\text{L}_4]^{2-}$ cluster that is based on a Fe_4S_4 core and contains five-coordinate, FeS_5 , iron sites is the $[\text{Fe}_4\text{S}_4(\text{S}_2\text{C}_2(\text{CF}_3)_2)_4]^{2-}$ cluster.¹⁵ In this cluster the geometry of the FeS_5 units is trigonal bipyramidal.

Preliminary Mössbauer measurements on I at 77 K show two absorptions for the structurally distinct iron sites with isomer shifts (IS) and quadrupole splittings (QS) of 0.39, 1.34 mm/s and 0.74, 1.67 mm/s (vs. Fe at 298 K). The first set of these parameters are similar to the IS and QS of the single resonance in $[\text{Fe}_4\text{S}_4(\text{SPh})_4]^{2-}$ at 0.42 (1) and 0.94 (1) mm/s. The second set of values very likely is associated with the iron atoms coordinated by the Et_2dtc ligands. The isomer shift of 0.74 mm/s differs substantially from the values reported for

- (6) Reynolds, J. G.; Laskowski, E. J.; Holm, R. H. *J. Am. Chem. Soc.* **1978**, *100*, 5315.
 (7) The magnetic susceptibility of the cluster shows $\mu_{\text{eff}}^{\text{cor}} = 2.56 \mu_{\text{B}}$, measured by the NMR method in $\text{Me}_2\text{SO}-d_6$ at 300 K.
 (8) Crystal and refinement data for $(\text{Ph}_4\text{P})_2[\text{Fe}_4\text{S}_4(\text{SPh})_2(\text{Et}_2\text{dtc})_2]$: $a = 17.486$ (3) Å, $b = 18.240$ (3) Å, $c = 24.198$ (3) Å, $\beta = 109.73$ (1)°; space group $C2/c$ (No. 15); $Z = 4$; $d_{\text{calcd}} = 1.41 \text{ g/cm}^3$, $d_{\text{obsd}} = 1.40$ (2) g/cm^3 ; crystal dimensions (mm) $1.16 \times 0.22 \times 0.22$; $\mu = 11.6 \text{ cm}^{-1}$; $2\theta_{\text{max}} 50^\circ$ (Mo, $\lambda(\text{K}\alpha_1) 0.70926$ Å); unique reflections collected 5941; reflections used in refinement, $F_o^2 > 3\sigma(F_o^2)$, 3226; parameters 661. All crystal data were collected at ambient temperature on a recently purchased XRD P3/F Nicolet four-circle diffractometer, controlled by a Data General NOVA 3 computer. The structure was solved by direct methods using the program MULTAN (1971) and by subsequent Fourier electron density maps. The air-sensitive crystal was sealed inside a 0.3-mm i.d. quartz capillary tube. In the refinement process for I by full-matrix least-squares techniques, anisotropic temperature factors were employed for all non-hydrogen atoms in the asymmetric unit. Hydrogen atoms were input at their calculated positions (0.95 Å from the carbon atom) and used in the structure factor calculations but were not refined. At the present stage of refinement $R = 0.078$.
 (9) Averill, B. A.; Herskovitz, T.; Holm, R. H.; Ibers, J. A. *J. Am. Chem. Soc.* **1973**, *95*, 3523.

- (10) The S atom positional deviations from the unweighted least-squares plane range from -0.15 (1) to $+0.14$ (1) Å.
 (11) Hoskins, B. F.; White, A. H. *J. Chem. Soc. A* **1970**, 1668.
 (12) Ileruma, O. A.; Feltham, R. D. *Inorg. Chem.* **1975**, *14*, 3042.
 (13) Coucouvanis, D. *Prog. Inorg. Chem.* **1979**, *26*, 301.
 (14) If the midpoint of the Et_2dtc sulfur atoms is considered as one coordination site, the distorted tetrahedral coordination around Fe_2 will be characterized by tetrahedral angles that range from 105.9 (3) to 123.5°.
 (15) Bernal, I.; Davis, B. R.; Good, M. L.; Chandra, S. *J. Coord. Chem.* **1972**, *2*, 61–65.

either the five-coordinate Fe(III) in $\text{ClFe}(\text{Et}_2\text{dtc})_2^{16}$ (0.50 mm/s, 100 K vs. Fe) or the five-coordinate Fe(II) in the $[\text{Fe}(\text{Et}_2\text{dtc})_2]_2$ dimer¹⁶ (0.90 mm/s, 100 K vs. Fe).

The voltammetry of I in DMF¹⁷ shows both a reduction wave at -1.2 V and an oxidation wave at -0.07 V. Quantitative studies of these waves by chronoamperometry show both the oxidation and the reduction to be diffusion controlled over the range of 20 ms-1 s. The current functions $i_c t^{1/2}/C$ and $i_a t^{1/2}/C$ for the reduction and oxidation, respectively, correspond to one-electron processes. The reduction wave shows no associated anodic wave, and the reduction product appears completely unstable. The oxidation wave is accompanied by a small cathodic wave. The i_c/i_a ratio in double potential step chronoamperometry shows the oxidation product to be stable for about 100 ms. A significant decline in this ratio is observed at longer potential steps ($i_c/i_a = 0.16$, $t = 1$ s).

The $[\text{Fe}_4\text{S}_4\text{L}_4]^{2-}$ clusters generally undergo reversible one-electron reductions. The apparently different redox properties of I must be attributed mainly to the Et_2dtc^- ligand. The latter is known to stabilize highly oxidized states in simple $\text{M}(\text{Et}_2\text{dtc})_n$ complexes.¹³ The effects of terminal ligand coordination characteristics in the redox properties of the $[\text{Fe}_4\text{S}_4\text{L}_4]^n$ clusters at present are not well understood. A systematic study of the molecular and electronic structures and redox properties of various "mixed" terminal ligand clusters is under way in our laboratory.

Acknowledgment. This research was supported by a grant from the National Institutes of Health (No. GM-26671-03). X-ray equipment used in this research was obtained in part by Grant CHE-8109065 from the National Science Foundation.

Registry No. I, 83692-59-5; $(\text{Ph}_4\text{P})_2[\text{Fe}_4\text{S}_4(\text{SPh})_2\text{Cl}_2]$, 80939-30-6; $(\text{Ph}_4\text{P})_2[\text{Fe}_4\text{S}_4(\text{SPh})_4]$, 80765-13-5.

Supplementary Material Available: Tables of structure factors and positional and thermal parameters (26 pages). Ordering information is given on any current masthead page.

(16) De Vries, J. L. K. F.; Keijzers, C. P.; De Boer, E. *Inorg. Chem.* 1972, 11, 1343.

(17) The electrochemical studies were conducted in DMF solution (0.1 M) in *n*-Bu₄NClO₄ on a Pt electrode vs. a saturated calomel reference electrode.

(18) Johnson, C. K. Report ORNL-3794; Oak Ridge National Laboratory; Oak Ridge, TN, 1965.

Department of Chemistry
University of Iowa
Iowa City, Iowa 52242

M. G. Kanatzidis
M. Ryan
D. Coucouvanis*

Nuclear Research Center "Demokritos"
Aghia Paraskevi, Attiki, Greece

A. Simopoulos
A. Kostikas

Received August 2, 1982

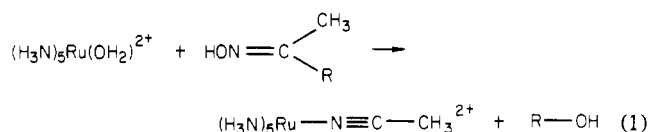
Spontaneous Carbon-Carbon Bond Cleavage of Some Ruthenium(II)-Bound α -Substituted Ketoximes

Sir:

We report the first example of C-C bond cleavage in a ligand attached to ruthenium(II) that is not accompanied by an oxidation-reduction reaction.¹

The reaction, which occurs when $(\text{H}_3\text{N})_5\text{RuOH}_2^{2+}$ is generated² in the presence of a ketoxime containing an α -keto or

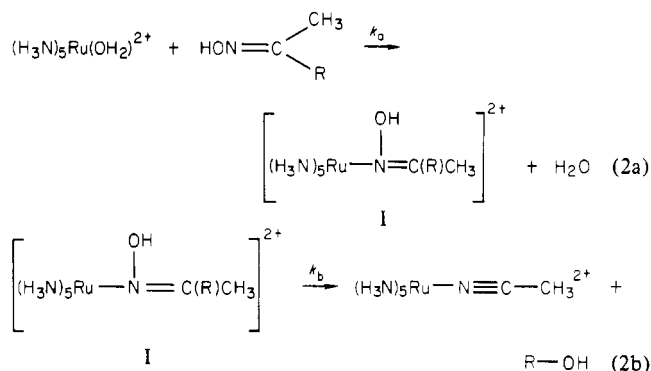
α -hydroxy group, has the overall stoichiometry



where R is $-\text{C}(\text{O})\text{CH}_3$, $-\text{C}(\text{O})\text{C}_6\text{H}_5$, or $-\text{CH}(\text{OH})\text{C}_6\text{H}_5$.

The ruthenium(II)-nitrile products were isolated as the perchlorate salts and identified by comparison of their UV-vis and IR spectra with those of authentic samples.³ Benzoic acid was recovered and identified (proton NMR and IR spectra and melting point) in the $\text{R} = \text{C}(\text{O})\text{C}_6\text{H}_5$ case, and benzaldehyde was identified (proton NMR) in the $\text{R} = \text{CH}(\text{OH})\text{C}_6\text{H}_5$ case.

Since these oximes do not normally decompose in aqueous solutions and ligand substitution for H_2O in $(\text{H}_3\text{N})_5\text{Ru}-\text{OH}_2^{2+}$ is rapid,⁴ the reaction must involve the two steps shown in eq 2.



Attempts to isolate or detect the presence of the proposed ruthenium(II)-oxime intermediate, I, were unsuccessful, suggesting that the rate of disappearance of I is fast compared to its rate of formation. This remarkable increase in the reactivity of the oxime ligand in the absence of a concurrent redox change provides unambiguous evidence for the ability of Ru(II) to promote increased unsaturation on bonded nitrogen atoms, a phenomenon generally attributed to strong back-bonding from the filled 4d orbitals on Ru(II) to the empty π^* orbitals on sp^2 - or sp -hybridized nitrogen.⁵

Reactions were carried out at about 25 °C in dilute solution (~ 0.01 M in Ru and ~ 0.02 M in oxime).

A lower limit of 0.020 s^{-1} can be estimated for k_b if it is assumed (a) that $[\text{I}] < [\text{Ru}_{\text{total}}]/10$, (b) that k_a is similar to that for other sp^2 -hybridized ligands⁴ (average of seven neutral unhindered ligands $0.10 \text{ M}^{-1} \text{ s}^{-1}$, range 0.05 - $0.20 \text{ M}^{-1} \text{ s}^{-1}$), and (c) that reaction 2b is first order.

Related studies on aldoximes and unsubstituted oximes will be reported elsewhere.

Acknowledgment. This research was supported in part by the Metal Loan Program of Johnson Matthey, Inc.

Registry No. $(\text{H}_3\text{N})_5\text{Ru}(\text{OH}_2)^{2+}$, 21393-88-4; $\text{HON}=\text{C}(\text{CH}_3)-\text{C}(\text{O})\text{CH}_3$, 57-71-6; $\text{HON}=\text{C}(\text{CH}_3)\text{C}(\text{O})\text{C}_6\text{H}_5$, 119-51-7; $\text{HON}=\text{C}(\text{CH}_3)\text{CH}(\text{OH})\text{C}_6\text{H}_5$, 26226-58-4; $(\text{H}_3\text{N})_5\text{RuN} \equiv \text{CCH}_3^{2+}$, 26540-31-8; HOAc, 64-19-7; benzoic acid, 65-85-0; benzaldehyde, 100-52-7.

(2) $(\text{H}_3\text{N})_5\text{RuOH}_2^{2+}(\text{aq})$ is prepared from $[(\text{H}_3\text{N})_5\text{RuCl}]\text{Cl}_2$ (A. D. Allen and C. V. Senoff, *Can. J. Chem.*, 45, 1337 (1967)) by treatment with $\text{Ag}^+(\text{aq})$ or $\text{OH}^-(\text{aq})$ followed by amalgamated zinc.

(3) P. C. Ford and R. E. Clarke, *Inorg. Chem.*, 9, 227-35 (1970).

(4) R. E. Sheperd and H. Taube, *Inorg. Chem.*, 12, 1392-401 (1973).

(5) (a) P. C. Ford, *Coord. Chem. Rev.*, 5, 77-99 (1970); (b) H. Taube, *Surv. Prog. Chem.*, 6, 1-46 (1973).

Department of Chemistry
Illinois Institute of Technology
Chicago, Illinois 60616

Charles P. Guengerich
Kenneth Schug*

Received September 16, 1982

(1) $\text{Ru}(\text{NH}_3)_5\text{NO}^{3+} + \alpha$ -methylene ketones: K. Schug and C. P. Guengerich, *J. Am. Chem. Soc.*, 101, 235-6 (1979). Other types of enhanced ligand reactivity also are accompanied by net redox changes.